

Tailorable polymer waveguides for miniaturized bio-photonic devices via two-polymer microtransfer molding

Jae-Hwang Lee^{1,3}, Zhuo Ye^{1,3}, Kristen Constant^{2,3}, and Kai-Ming Ho^{1,3}

1. Department of Physics and Astronomy, Iowa State University, Ames, Iowa 50011, USA
2. Department of Materials Science and Engineering, Iowa State University, Ames, IA 50011, USA
3. Ames Laboratory, U.S. Department of Energy, Ames, IA 50011, USA

ABSTRACT

Traditional optical fibers have been developed to achieve novel characteristics for both macro- and micro-applications. Inorganic optical waveguides using two-dimensional photonic crystals and silicon-on-insulator technology are examples of recent trends for macro- and micro-scale optical applications, respectively. As bio-photonics devices operate mostly with visible light, visible-transparent materials such as metal oxides and polymers are preferred as the guiding medium. Although polymers have tremendous potential because of their enormous variation in optical, chemical and mechanical properties, their application for optical waveguides is limited by conventional lithography. We present a non-optical lithographic technique, called two-polymer microtransfer molding, to fabricate polymer nano-waveguides, on-chip light sources and couplers. Micro-sources using quantum dots emitting red light (625nm) are successfully embedded in a waveguides array as the on-chip light sources. Fabrication of a grating coupler is also attempted for various external light sources including lasers and white light. We have quantified propagation losses of the waveguides using CCD photometry. The guiding loss is approximately 1.7dB/mm. We also demonstrated that the surface roughness of the fabricated waveguides can be reduced by chemical etching. We demonstrate that low cost, high yield, high fidelity, and tailorable fabrication of bio-photonic devices are achievable by the combination of the presented techniques.

Keywords: Polymer waveguide, Microfabrication, Soft lithography, Microtransfer molding, Grating coupler, Guiding loss

1. INTRODUCTION

Miniaturized photonic devices consisting of waveguides, couplers and light sources are in great demand for bio-applications [1,2,3,4]. In addition to their functionality, low cost is advantageous especially for disposable devices which are desirable for avoiding contamination and long preparation times. Additionally, polymers are considered to be promising materials for biophotonic applications because of their processability, cost-effectiveness, high yield and wide tenability [5]. To develop miniaturized photonic devices, the fabrication of optical waveguides is crucial since highly integrated novel functionalities depend on a well-organized optical network. To fabricate the polymer waveguides, various techniques, such as reactive ion etching [6], laser direct writing [7], nano-imprinting [8], direct drawing [9], replica molding [10], and microtransfer molding [11], have been developed. Among them, microtransfer molding (μ TM) has a number of capabilities making it well-suited for low-cost, non-planar and three-dimensional (3D) fabrication of polymer waveguides. Recently, we have developed an advanced microtransfer molding technique, called two-polymer microtransfer molding (2P- μ TM) [12], which shows high yield and good quality in 3D layer-by-layer fabrication. Moreover, 2P- μ TM is expected to enable mass production of bio-photonic devices by roll-to-roll fabrication.

2. EXPERIMENTAL

2.1 Fabrication of a waveguide array and light sources

In 2P- μ TM (see Figure 1), a photo-curable polyurethane prepolymer (J-91, Summers Optical) is filled in micro-patterns of a poly(dimethylsiloxane) (PDMS)-based elastomeric mold and solidified. The surface of pre-filled polymer is coated with a photo-curable polymetacrylate prepolymer (SK-9, Summers Optical) as an adhesive layer and is placed in contact with a substrate. By peeling off the elastomeric mold after curing the adhesive layer, micro-elements in the patterns are

transferred to the substrate. In this article, we demonstrate that 2P- μ TM can be applied to fabricate micro-waveguides with physical dimensions that are comparable to the wavelength of guided light. Such small waveguides are in high demand for bio-sensing since the guided light can interact with surrounding biological entities [13].

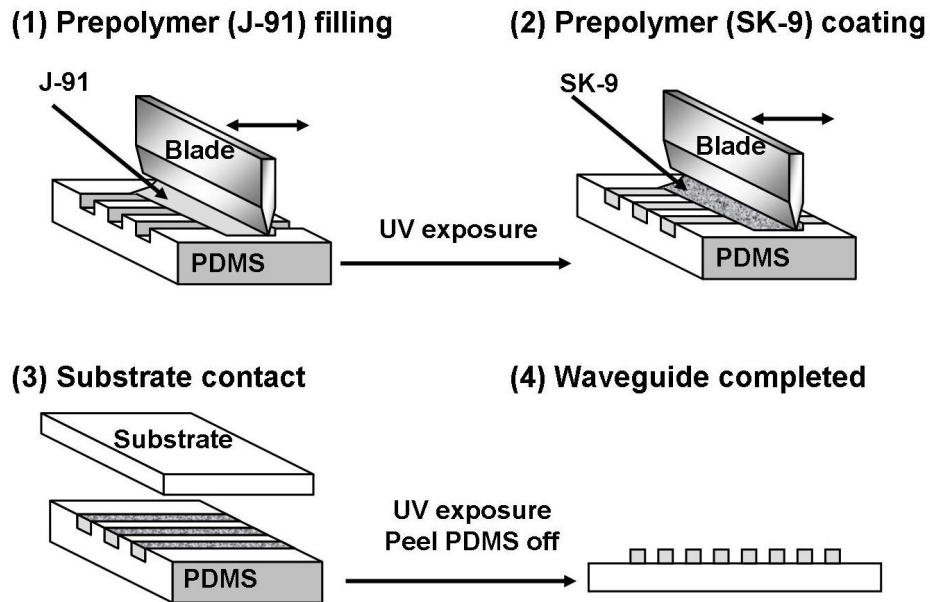


Fig. 1. Schematic illustration of 2P- μ TM for waveguides

An array of waveguides is fabricated on an oxidized silicon substrate, with a $2.0\ \mu\text{m}$ thick oxide layer, as seen in Figure 2a. The cross section of the fabricated waveguide is slightly trapezoidal rather than rectangular with a height of $1.2\ \mu\text{m}$, and a base of $1.3\ \mu\text{m}$, and a top of $1.0\ \mu\text{m}$. The distance between two adjacent waveguides is $2.5\ \mu\text{m}$. Since the refractive indices of the waveguides and the oxide layer are 1.55 [14] and 1.46 [15], respectively, their contrast is sufficient for light guiding. A waveguide structure fabricated by other soft lithographic techniques like replica molding or conventional μ TM [16] often has an undesirable residual layer between waveguides which may potentially limit the functionality of the waveguides. Although the residual layer can be reduced by dilution of the material for waveguides [17] or can be removed by reactive ion etching after fabrication [18], the best way to accomplish this is with a fabrication method such like 2P- μ TM, that does not result in a residual layer.

The coupling of light source to a waveguide is a critical issue for practical applications. Several coupling methods including direct focusing, butt coupling, prism, and grating coupling, have been developed [19], however, we used direct embedding of light sources on waveguides for simplicity of fabrication and ease of alignment. As high dosage of ultraviolet (UV) is usually used in 2P- μ TM for waveguide fabrication, UV-resistant inorganic light-emitting materials are preferred. Since high efficiency semiconductor quantum dots (QDs) are commercially available, we used a UV-curable QD resin (Evident Tech.) without modification for compatibility with 2P- μ TM. As seen in Figure 2b, $0.1\ \text{nano-liter}$ of the QD resin is applied on the desired position of the fabricated array of waveguides using a metallic stylus. After application, the QD resin slightly spreads along the direction of the waveguides until it is solidified by UV exposure. Here, we anticipate that the light from the QDs by photo-excitation will couple to the guiding modes of the waveguides as illustrated in Figure 2c.

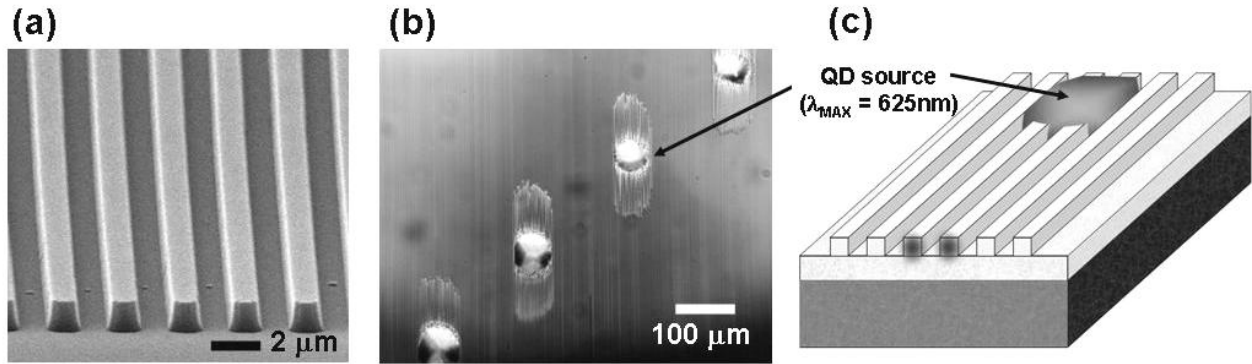


Fig. 2. Fabricated waveguides array with coupled light sources. (a) SEM micrograph of the waveguides and (b) optical micrograph of the coupled light sources are shown with (c) a schematic illustration of guided light.

2.2 Numerical calculation for the waveguides

Numerical calculations were performed to predict the mode diagram and profiles of each mode of the fabricated trapezoidal waveguides. The plane wave based transfer matrix method (TMM) is used for those calculations [20,21]. A supercell of $2.5 \mu\text{m} \times 5.0 \mu\text{m}$ and 29×29 plane waves were used. To distinguish each mode clearly, the difference between the z-component of the wave vector of guiding modes and the magnitude of the wave vector of the leaky mode through the oxide layer, $(h/2\pi)[k_z - k_0 n_s]$, versus the normalized frequency, $\omega h/2\pi c$, is plotted in Figure 3a, where h , n_s and c are the height of the waveguide, the refractive index of the oxide layer and speed of light in vacuum, respectively. In the numerical calculations, the silicon below the oxide layer is also considered; however, a guiding mode through the homogeneous oxide layer does not exist due to the high absorptance of silicon. Because of asymmetry of the waveguides, two similar modes appear in each band. For the maximum emission wavelength of the QDs ($\lambda_{\text{MAX}}=625$ nm), we can see that two very similar fundamental modes exist and their electric fields are well confined in the waveguide as shown in Figure 3b. Two more modes at higher frequencies is also shown in Figure 3c although their fields extend into the substrate considerably because the thickness of oxide layer is large ($2 \mu\text{m}$). In contrast, the mode in Figure 3d barely exists so it cannot be a major guiding mode. From the numerical calculation, we can assume that the four lowest modes having the profiles in Figure 3b and 3c play the major role in propagation of light.

2.3 Characteristics of the waveguides

In addition to numerical calculations, we experimentally investigated the guiding characteristics of the waveguide array with the QD sources. The QD source is excited by a focused Argon ion laser ($\lambda=365$ nm) and the guided light is collected by an optical fiber with a core diameter of $100 \mu\text{m}$ (see Figure 4c). Since a single QD source is coupled to approximately 30 individual waveguides as seen Figure 2b, the collected light is the sum of all guided light through the source-coupled waveguides (see Figure 4d). In Figure 4a, the emission spectrum of the QD dots and the spectrum of guided light are shown for comparison. Because the two spectra can be shifted by changing the distance to the collecting fiber, the values of the relative intensity in Figure 4b do not completely represent the guiding loss and coupling efficiency; however, we see the fabricated waveguides show a flat guiding behavior around the emission region. This neutral response of the waveguides will be useful for light delivery to a desired point without altering the source spectrum.

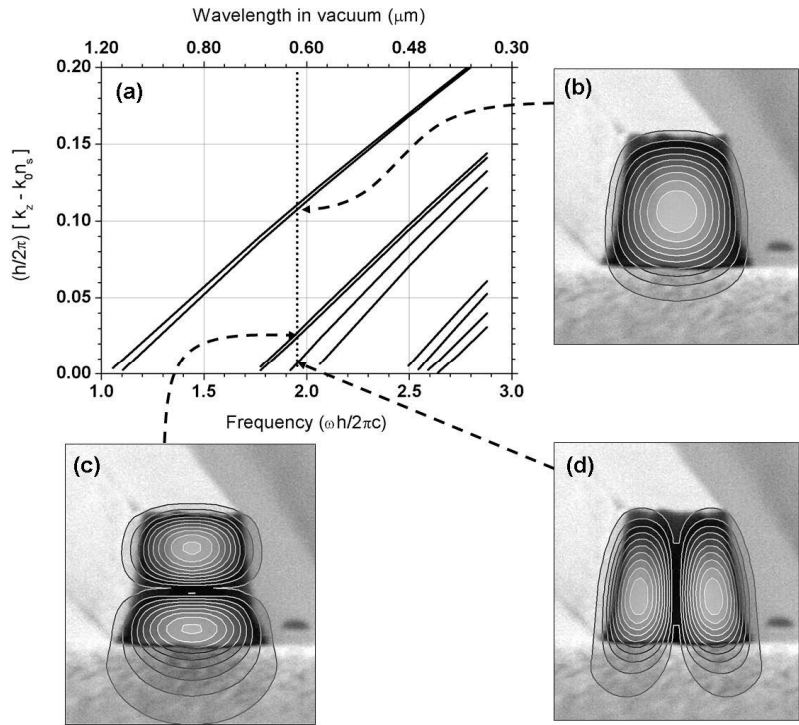


Fig. 3. The calculated mode diagram is shown with three selected electric field profiles for $\lambda = 625$ nm. The calculated electric field profiles are superimposed on a SEM micrograph of a single waveguide.

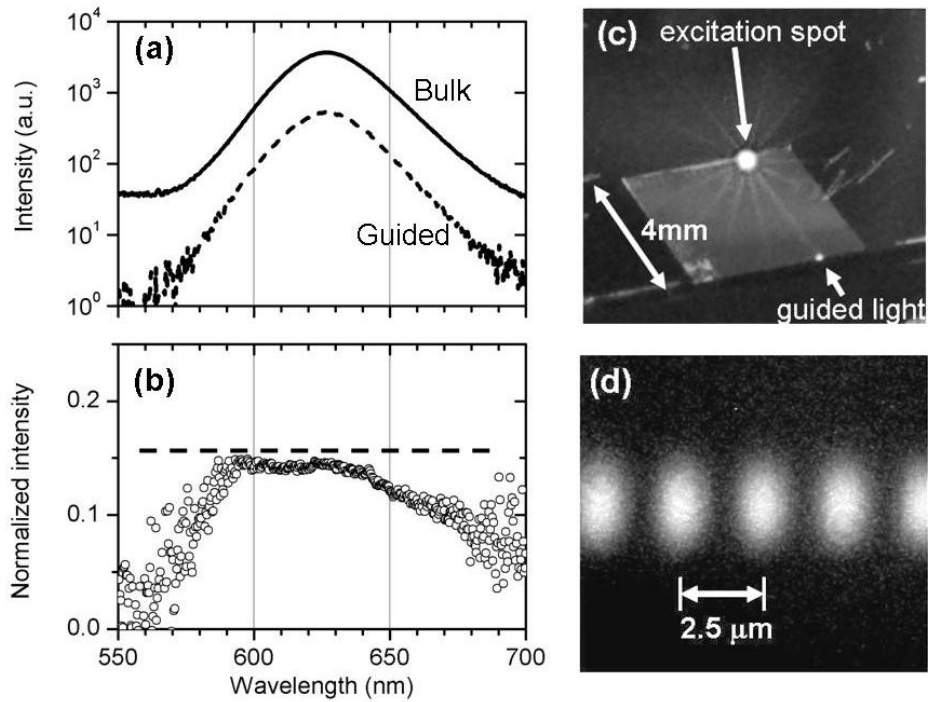


Fig. 4. Guiding characteristics of the waveguides (a) Emission spectrum of the bulk quantum-dots resin and the optical spectrum after guiding; (b) Relative intensity between the two spectra; (c) Photograph of the waveguide array during the measurement; (d) Optical micrograph of guided light

The guiding loss of the waveguides has been experimentally quantified. Because of the small size of the waveguides, we estimate the guiding loss by photometry using a microscopic charge-coupled device (CCD) camera. Compared to the guiding loss of conventional communication optical fibers, that of micro-waveguides is significantly larger, on the order of 1dB/mm. Therefore, we can directly detect the leaky light by a microscopic CCD camera. The optical field of the camera is corrected to be flat by using a reference image of a flat field from an integrating sphere, and dark current contribution is also compensated [22]. All data acquisition is performed in the linear regime of the CCD camera. Figure 5b is the acquired image after all corrections. The guided light propagates from left to right. In the image, all source-coupled waveguides appear as a single bright region rather than individual waveguides. The bright area contains approximately 30 waveguides directed from left to right. In contrast, other areas are significantly darker because the waveguides in those areas are not coupled with the QD light source. The distinct bright spots represent relatively large leaks of the guided light caused by defects of the waveguides and tiny dust particles on the surface of the waveguides. The intensities of the pixels in the source-coupled region and in the uncoupled region are averaged, respectively, along the y-axis. Figure 5a shows the difference between the two average values along x-axis. A number of peaks in the averaged difference are from the localized bright spots. From an exponential decay fitting of the baseline, we can determine a decay coefficient, 0.4 which corresponds to a guiding loss of 1.7dB/mm. This value is comparable to that of other small waveguides [8,23,24].

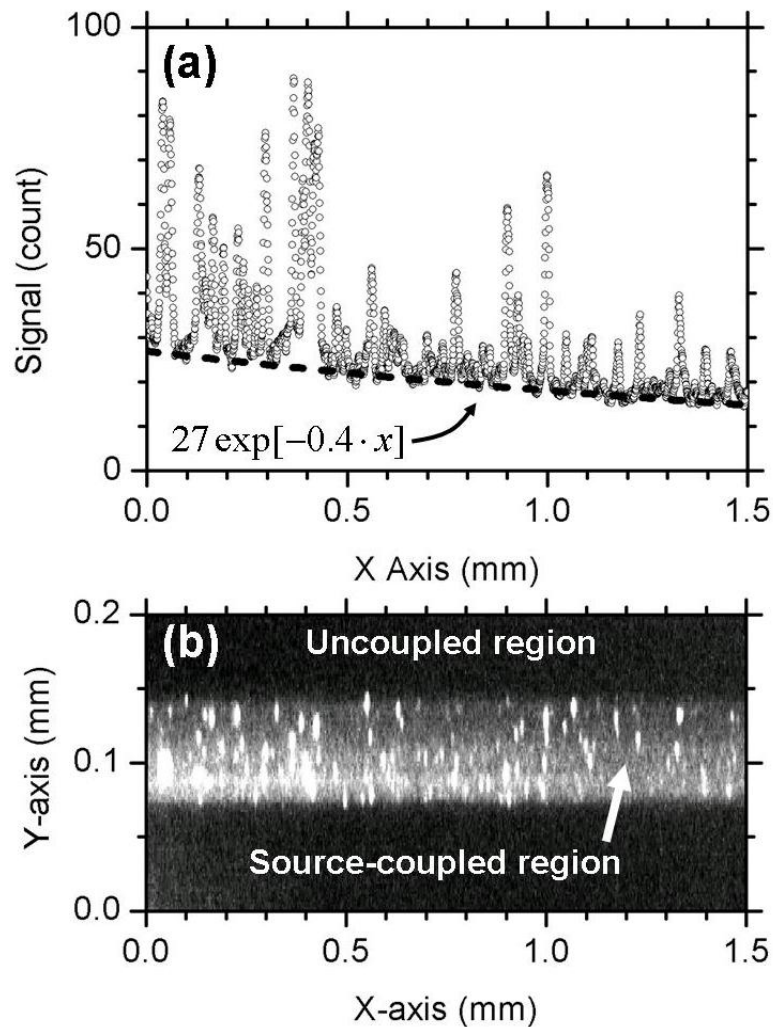


Fig. 5 Quantification of the guiding loss by photometric imaging. (a) average value of pixels, perpendicular to the waveguiding direction; (b) acquired image data after all corrections for photometry.

2.4 Grating coupler

The direct embedding of a QD source enables simple and compact source coupling without requiring accurate alignment, however, an external source coupling is still desirable, mostly for high intensity applications. Since 2P- μ TM is superior for layer-by-layer fabrication, fabricating a grating coupler is technically simpler than in other techniques. However, fabrication of a grating coupler for visible light is also a technical challenge since the grating coupler requires a sub-micron feature size, and this scale has not been reported before. Because of the high yield of 2P- μ TM, it is possible to transfer a grating structure to the top of a fabricated waveguide array using the same procedure in Fig. 1. A fabricated grating coupler is seen on top of an array of waveguides in Figure 6a and 6b. The periodicity of the grating is $1.0\ \mu\text{m}$ and each bar of the grating is $0.5\ \mu\text{m}$ wide and $0.6\ \mu\text{m}$ high. Because of the additive nature of 2P- μ TM, the grating coupler can be added without any etching processing. To find an efficient incident angle, a Helium-Neon laser beam ($\lambda=633\ \text{nm}$) is focused on the edge of the grating coupler and the angle to the surface normal is changed while monitoring the guided light. At the incident angle of around 60° , the most intense guided light is observed in Fig. 6c. Instead of the laser beam, white light from a tungsten lamp can also be coupled to the waveguides with the grating coupler. We observe different colors of guided light from changing from red to blue with changing incident angle.

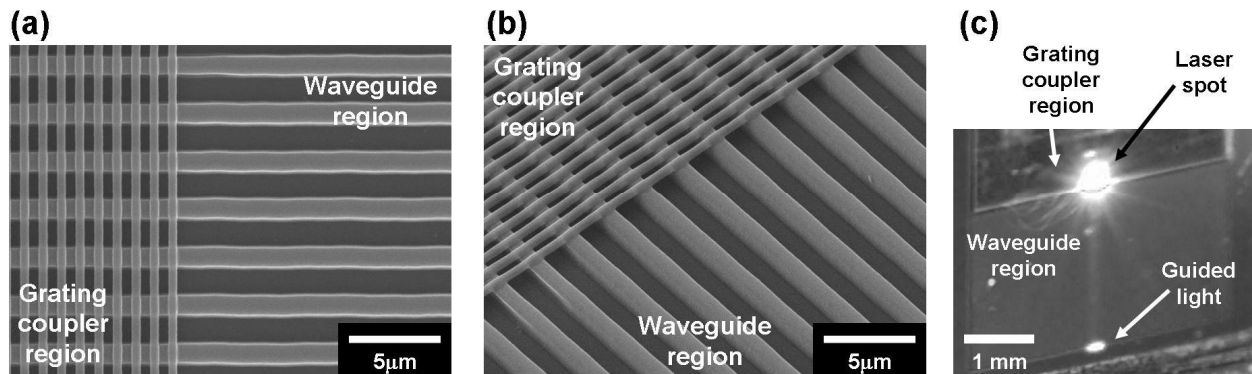


Fig. 6. Fabricated grating coupler. (a) Top and (b) slant view of the SEM micrographs of the grating coupler; (c) Photograph of the waveguide array with the grating coupler shows the guided light.

2.5 Additional etching procedure to modify the surface roughness of waveguides

The surface roughness of waveguides is a major cause of guiding loss. Both side walls of waveguides by 2P- μ TM are rougher than the top because side wall roughness originates from the etched features of a master pattern which is used for the casting of the PDMS molds. Since the polyurethane does not flow under heat, considerable chemical etching is required to reduce the surface roughness; however, the chemical stability of the polyurethane makes it difficult to find a suitable etchant. We found a potassium hydroxide (KOH) aqueous solution can be used as the etchant for the polyurethane. To have an appropriate etching rate, we used a 5 wt% KOH solution at a room temperature. Fig. 7 shows the result of the KOH etching for 15 seconds and the corresponding etching rate is $10\ \text{nm/sec}$ approximately. Etching longer than 15 seconds often causes the detachment of the waveguides from their substrate. This is possibly because of etching of silica by the KOH solution. Although longer etching time is not possible due to the detachment, we observed the surface morphology could be modified sufficiently within a short time. The SEM micrographs in Fig 8 show the change of the surface roughness of the waveguides by the etching. The surface of the side wall is apparently smoother than before etching and the guiding loss is expected to be reduced by the smoothing.

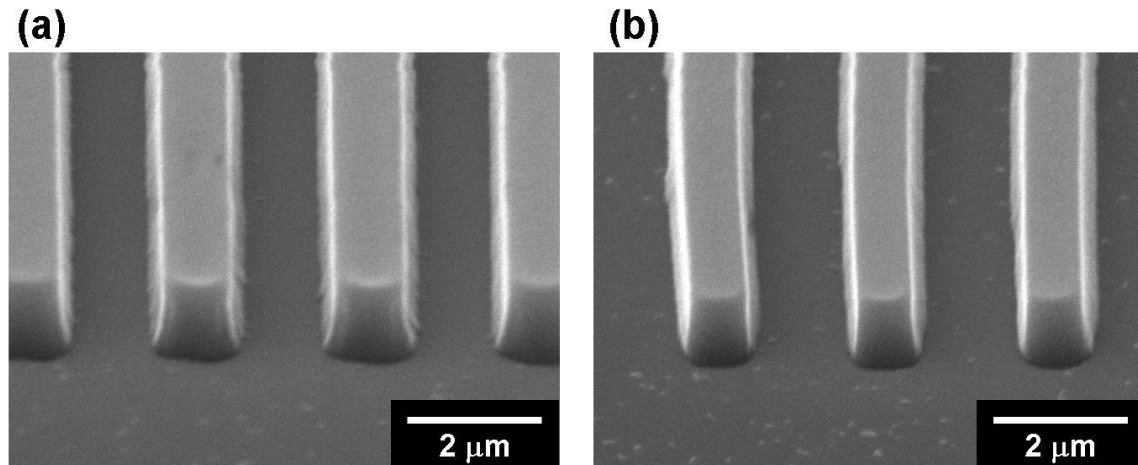


Fig. 7. Comparison of waveguides (a) before and (b) after the KOH etching.

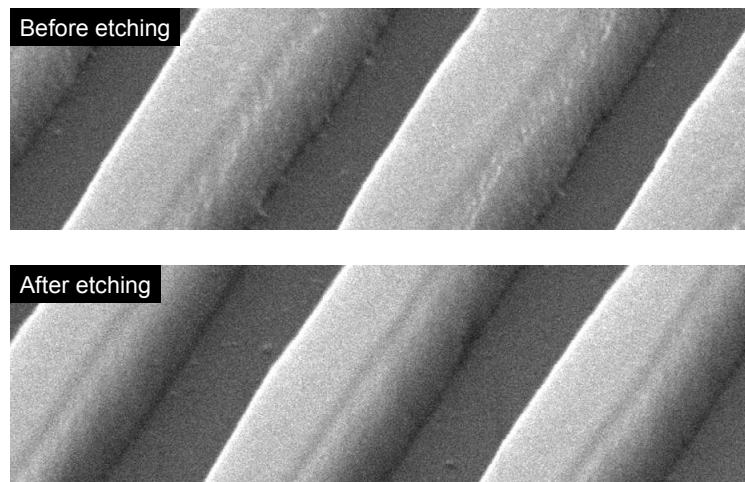


Fig. 8 Comparison of sidewall of waveguides before and after the KOH etching.

3. CONCLUSION

A non-photolithographic fabrication technique, called 2P- μ TM, is applied to produce small polymer waveguides. The fabricated waveguides show sufficient performance to be used for photonic devices in the visible regime with a guiding loss of 1.7dB/mm. Two different source coupling methods are demonstrated for internal and external light sources. The light from the embedded QD light source is efficiently coupled to the waveguides and this coupling would be useful for miniaturized sensing devices in bio-applications even under aqueous solutions. In addition, a grating coupler for an external light source is also successfully demonstrated indicating that 2P- μ TM has sufficient structural fidelity even for submicron features. Moreover, we expect that the demonstrated guiding loss can be reduced by the chemical etching of the fabricated polymer waveguides using the KOH aqueous solution.

ACKNOWLEDGEMENTS

This work is supported by the Director for Energy Research, Office of Basic Energy Sciences. The Ames Laboratory is operated for the U. S. Department of Energy by Iowa State University under Contract No. W-7405-ENG-82. One of the authors (Z.Y.) acknowledges Ming Li for helpful assistance in the numerical calculations.

REFERENCES

1. R. E. Kunz, "Miniature integrated optical modules for chemical and biochemical sensing" *Sens. Actuators B*, **38**, 13 (1997).
2. R. Horváth, L. R. Lindvold, N. B. Larsen, "Reverse-symmetry waveguides: theory and fabrication" *Appl. Phys. B* **74**, 383 (2002).
3. J. Vörös, J. J. Ramsden, G. Csúcs, I. Szendrő, S. M. De Paul, M. Textor, N. D. Spencer, "Optical grating coupler biosensors" *Biomaterials* **23**, 3699 (2002).
4. D. A. Chang-Yen, B. K. Gale, "An integrated optical oxygen sensor fabricated using rapid-prototyping techniques" *Lab on a Chip* **3**, 297 (2003).
5. H. Ma, A. K. -Y. Jen, L. R. Dalton, "Polymer-based optical waveguides: materials, processing, and devices" *Adv. Mater.* **14**, 1339 (2002).
6. J. H. Kim, E. J. Kim, H. C. Choi, C. W. Kim, J. H. Cho, Y. W. Lee, B. G. You, S. Y. Yi, H. J. Lee, K. Han, W. H. Jang, T. H. Rhee, J. W. Lee, S. J. Pearton, "Evaluation of fluorinated polyimide etching processes for optical waveguide fabrication", *Thin Solid Films* **341**, 192 (1999).
7. A. K. Das, "Laser direct writing polymeric single-mode waveguide devices with a rib structure" *Appl. Opt.* **42**, 1236 (2003).
8. J. Seekamp, S. Zankovych, A. H. Helfer, P. Maury, C. M. Sotomayor Torres, G. Böttger, C. Liguda, M. Eich, B. Heidari, L. Montelius, J. Ahopelto, "Nanoimprinted passive optical devices" *Nanotechnology* **13**, 581 (2002).
9. S. A. Harfenist, S. D. Cambron, E. W. Nelson, S. M. Berry, A. W. Isham, M. M. Crain, K. M. Walsh, R. S. Keynton, R. W. Cohn, "Direct drawing of suspended filamentary micro- and nanostructures from liquid polymers" *Nano Lett.* **4**, 1931 (2004).
10. G. T. Paloczi, Y. Huang, A. Yariv, J. Luo, A. K. -Y. Jen, "Replica-molded electro-optic polymer Mach-Zehnder modulator" *Appl. Phys. Lett.* **85**, 1662 (2004).
11. X. -M. Zhao, S. P. Smith, S. J. Waldman, G. M. Whitesides, M. Prentiss, "Demonstration of waveguide couplers fabricated using microtransfer molding" *Appl. Phys. Lett.* **71**, 1017 (1997).
12. J. -H. Lee, C. -H. Kim, K. -M. Ho, K. Constant, "Two-polymer microtransfer molding for highly layered microstructures" *Adv. Mater.* **17**, 2481 (2005).
13. D. J. Sirbully, M. Law, P. Pauzauskie, H. Yan, A. V. Maslov, K. Knusten, C. -Z. Ning, R. J. Saykally, P. Yang, "Optical routing and sensing with nanowire assemblies" *Proc. Natl. Acad. Sci.* **102**, 7800 (2005).
14. The value of the refractive index was acquired from Summers Optical, Inc.
15. H. R. Philipp, "*Handbook of Optical Constants of Solids (Ed. E. D. Palik)*", Academic (1985), pp749-763.
16. X. -M. Zhao, Y. Xia, G. M. Whitesides, "Soft lithographic methods for nano-fabrication" *J. Mater. Chem.* **7**, 1069 (1997).
17. G. T. Paloczi, Y. Huang, J. Scheuer, A. Yariv, "Soft lithography molding of polymer integrated optical devices: Reduction of the background residue" *J. Vac. Sci. Tech. B* **22**, 1764 (2004).
18. X. -M. Zhao, Y. Xia, G. M. Whitesides, "Fabrication of three-dimensional micro-structures: microtransfer molding" *Adv. Mater.* **8**, 837 (1996).
19. R. G. Hunsperger, "*Integrated Optics, 5th ed.*", Springer (2002), pp. 114-124.
20. Z. -Y. Li, K. -M. Ho, "Light propagation in semi-infinite photonic crystals and related waveguides structures", *Phys. Rev. B* **68**, 155101 (2003).
21. Z. -Y. Li, L. -L. Lin, K. -M. Ho, "Light coupling with multimode photonic crystal waveguides", *Appl. Phys. Lett.* **84**, 4699 (2004).
22. P. Martinez, A. Klotz, "*A Practical Guide to CCD Astronomy*", Cambridge (1998), pp.109-117.
23. C. -Y. Chao, L. J. Guo, "Thermal-flow technique for reducing surface roughness and controlling gap size in polymer microring resonators" *Appl. Phys. Lett.* **84**, 2479 (2004).
24. M. Law, D. J. Sirbully, J. C. Johnson, J. Goldberger, R. J. Saykally, P. Yang, "Nanoribbon waveguides for subwavelength photonics integration" *Science* **305**, 1269 (2004).